Self-confinement of a fast pulsed electron beam generated in a double discharge

2005 J. Phys. D: Appl. Phys. 38 2793

(http://iopscience.iop.org/0022-3727/38/16/008)

INSTITUTE OF PHYSICS PUBLISHING JOURNAL OF PHYSICS D: APPLIED PHYSICS

J. Phys. D: Appl. Phys. **38** (2005) 2793–2797 doi:10.1088/0022-3727/38/16/008

Self-confinement of a fast pulsed electron beam generated in a double discharge

H Goktas[1,6], M Udrea[2], Gulay Oke[3], A Alacakir[1], A Demir[4] and J Loureiro[5]

[1] Ankara Nuclear Research and Training Center, 06501, Besevler, Ankara, Turkey
[2] National Institute for Laser, Plasma and Radiation Physics, 76900 Bucharest, Romania
[3] Physics Department, Middle East Technical University, 06531 Ankara, Turkey
[4] Physics Department, University of Kocaeli, 41200 Kocaeli, Turkey
[5] Centro de Física dos Plasmas, Instituto Superior Técnico, 1049-001 Lisboa, Portugal

E-mail: goktas@photon.physics.metu.edu.tr

Received 18 October 2004, in final form 19 May 2005
Published 5 August 2005
Online at stacks.iop.org/JPhysD/38/2793

Abstract
The construction of a double discharge pulsed electron beam generator and the study of the characteristics of the beam are presented in this paper. The electron beam generator consists of a fast filamentary discharge in superposition with an ordinary glow discharge in low-pressure gases. The filling gas is argon or helium at approximately 0.1 Torr pressure. The duration of the electron beam is shorter than 50 ns and the peak current intensity is of the order of amperes. The electron density is evaluated by making use of Stark broadening of the H_β line and compared with the full computer simulation method. The pinch effect of the filamentary discharge is evaluated and its size compared with the diameter of the beam.

1. Introduction

Electron beams have many special properties which make them particularly well suited for use in materials handling. One of the most significant properties is that they can be positioned rapidly and accurately in space and time and are very suitable for use in completely automated processes. Intense focused electron beams are required in applications such as lithography, plasma processing and intense radiation sources. Besides thermo-ionic diodes or field emission diodes, plasma based high-brightness electron beams have been produced in different ways; either in a glow discharge [1] or in pseudospark devices [2] or by superposition of dc and pulsed discharge at low pressure [3, 4].

The double discharge pulsed electron beam generator (DDPEBG) is a device that allows generation of an intense electron beam by superposing two discharges, namely a low pressure dc glow discharge and a high current pulsed discharge. The experimental set-up basically consists of a 200 mm long quartz tube with 20 mm internal diameter and three hollowed, cylindrical electrodes each with 20 mm internal diameter and 100 mm long, positioned at some distance from each other. The first electrode, $K_{1,2}$, acts as a cathode for both the dc glow discharge and the pulsed one, the second electrode, A_2, acts as an anode to establish the glow discharge, while the third electrode, A_1, is used as a grounded anode for the pulsed discharge as shown in figure 1. The cathode and anode A_2 are separated by 50 mm, and the anode A_1 and A_2 by 150 mm. The inductances L insulate the dc power supply from the high voltage pulses. By using a coaxial cable a doubling voltage scheme is achieved and up to 40 kV high voltage pulse could be applied on the cathode.

If the high voltage pulse is applied to the electrodes when the dc glow discharge is operating, for specific values of current and pressure, a filamentary pulsed discharge is formed along the symmetrical axis of the tube. Within this filamentary discharge an intense electron beam is generated between the anode A_2 and A_1, while the high voltage pulse is applied between the common cathode $K_{1,2}$ and the anode A_1. Two ceramic very low inductance capacitors C are charged through the resistor R_2 and rapidly discharged through the gas by means of the spark gap and the coaxial cable.

A pulsed self-collimated intense electron beam, with a diameter of the order of a few microns, is then produced along the discharge tube axis using the synergy of the two discharges [5]. The beam is a few centimetres in length, up to 20 A peak current, 50 ns pulse duration and 70 Hz repetition

[6] Author to whom any correspondence should be addressed.

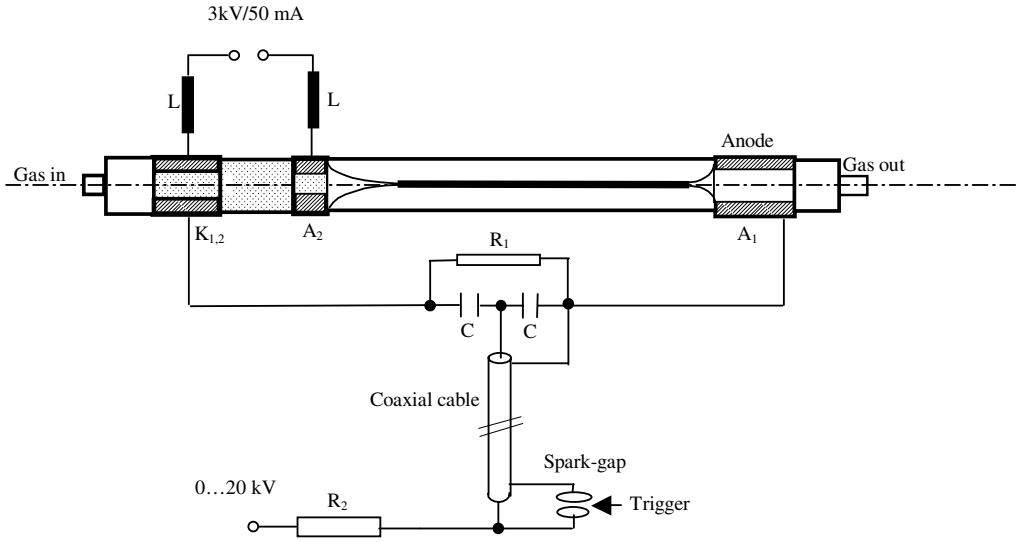

Figure 1. Experimental set-up of the DDPEBG ($R_1 = 110\,M\Omega$, $R_2 = 80\,M\Omega$, $C = 0.68\,nF$).

rate. The main discharge may be considered to be a hollow cathode discharge, similar to a pseudo-spark discharge that creates an intense electron beam, the propagation of which can be explained through the combined self-focusing action of both the magnetic field created by the electron beam and the radial space-charge electric field, with origin in the ionization of the gas, acting as a trap for the multiply charged ions.

2. Characteristics of the discharges

Higher plasma densities may be achieved using cylindrical hollow cathodes [6, 7]. This property combined with cylindrical symmetry gives rise to an optimum system for many applications. Although an important parameter of a cylindrical hollow cathode is its diameter d, there are a number of additional geometric parameters that influence the discharge characteristics, such as the cathode length, whether or not both extremities of the discharge are open, the aperture, the shape of the anode, the distance to it and the shape of the insulating walls. Experiments studying the effects of boundary conditions on the discharge characteristics, for which the hollow cathode effect is observed, the same effect as we have at our experimental set-up, are described in [8,9]. Those authors noticed that the discharge characteristics depend strongly on the ratio

$$\alpha = \frac{\text{(area of output aperture)}}{\text{(working surface of the cathode)}}. \qquad (1)$$

When α is smaller than 0.2 the discharge voltage is in the range $V_b = 200$–$500\,V$, whereas V_b increases rapidly as α increases, reaching the value $V_b \cong 1000\,V$ at $\alpha = 1.6$. The length of the hollow cathode electrode has been so chosen that the value of α is smaller than 0.2 and therefore allowing work with low breakdown voltages, V_b. The filling gas is argon. The I and V characteristics of the dc glow discharge are shown in figure 2. The vertical axis indicates the voltage, current intensity and plasma impedance, being the corresponding scales multiplied by different factors as is indicated on the insert of the figure. For a fixed dc applied voltage of 2.7 kV

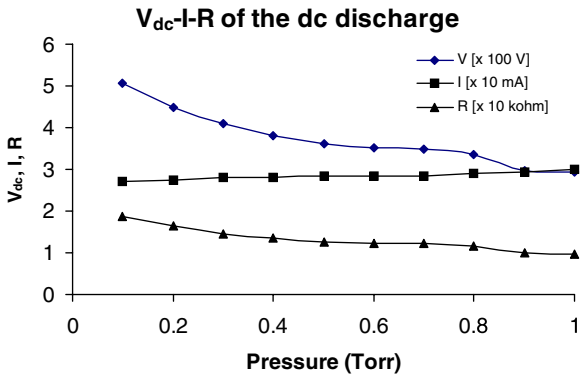

Figure 2. Variation of V_b, I and R in the dc discharge against the gas pressure.

the voltage drop on the tube varies between 293 and 505 V and the current between 30 and 27 mA as the pressure decreases in the range 1–0.1 Torr. An important observation is that the filamentary discharge occurs at relatively high impedances only, typically of the order of tenths of kΩ.

As mentioned above, the filamentary discharge occurs for specific pressure and voltage values of the pulsed discharge applied upon the operating dc glow discharge. The filamentary discharge lengths for different argon gas pressure and dc voltages are indicated in table 1. The filamentary discharge is ignited at a pressure of about 0.6 Torr and its length continuously increases as the pressure decreases to 0.1 Torr. We may hence consider that the dc hollow cathode glow discharge plays the role of a launcher for the pulsed electron beam, whereas the high voltage pulse strongly accelerates the electrons along the beam.

The voltage–current waveforms of the pulsed discharge are shown in figure 3. The high voltage was measured using a fast high voltage divider, while for the current we have used a home-made current shunt. This shunt was calibrated with respect to a Kenwood fast function generator. The waveforms were recorded by means of a Tektronix 620A oscilloscope. The voltage waveform depicted in figure 3 represents the anode

Table 1. Filamentary discharge length as a function of pressure and dc voltage.

Pressure (Torr)	1.0	0.9	0.8	0.7	0.6	0.5	0.4	0.3	0.2	0.1
Launcher, V_b (V)	293	297	337	347	351	361	382	409	450	505
Launcher, I_{dc} (mA)	30.0	29.5	29.0	28.5	28.5	28.5	28.0	28.0	27.5	27.0
Pulsed, V_p (kV)	12.0	12.0	12.0	12.0	12.0	12.0	12.0	13.6	14.4	15.2
Filament length (cm)	0	0	0	0	3	3.5	5.5	6.5	7.0	7.0

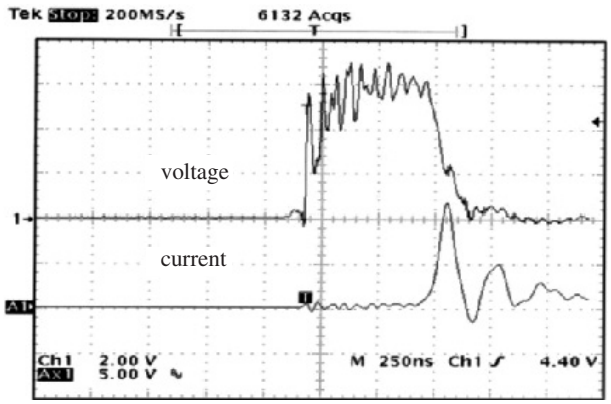

Figure 3. Typical voltage and current temporal behaviour of the pulsed discharge (for voltages each division indicates 2 kV and for current each division is 17 A).

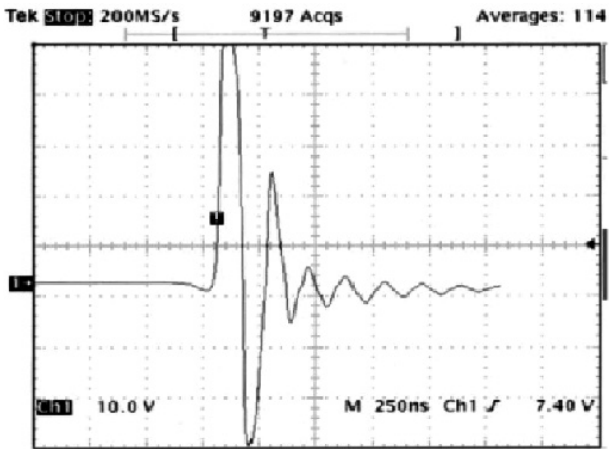

Figure 4. Electron beam current (each division is 0.12 A).

voltage evolution in the case of a 0.680 nF capacitor bank. The leading edge represents the increase of the voltage until the occurrence of the gas breakdown, whereas the break-off signal represents the end of the pulsed discharge. The maximum current intensity occurs at approximately half of the negative edge and the discharge peak current is found to be 41.0 A. All test devices have been inserted in the interior of a specially built Faraday cage which rejects the electromagnetic noise. Figure 3 shows that immediately after the breakdown voltage the impedance of the plasma presents a sharp decrease.

Figure 4 shows the total electron beam current collected by means of a Faraday cup. Here we believe that the first peak corresponds to the electron current in the discharge, while the second lower peak is due to secondary electrons emitted from the Faraday cup together with ions that surround the beam. The electron beam current is found to be $I_{beam} \cong 0.6$ A.

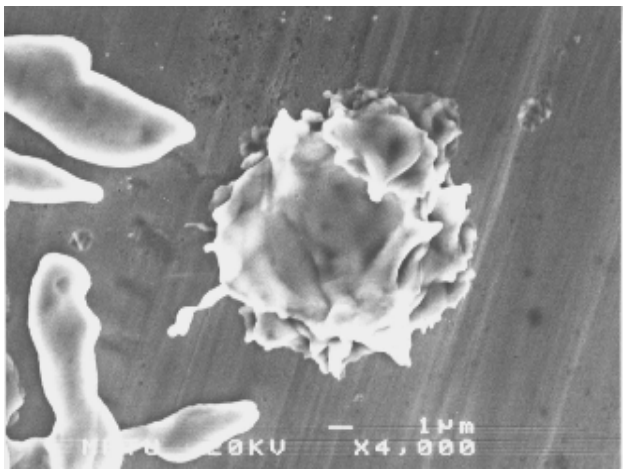

Figure 5. SEM picture of single shot on copper foil.

The diameter of the beam was measured by inserting a copper foil in front of the anode of the pulsed discharge in order to simulate the effect of one pulse on the target. The scanning electron microscope (SEM) picture of a single shot on the copper foil is shown in figure 5. The diameter of the beam has been evaluated as $\sim 8\ \mu$m. In the following sections we will compare this value with the beam diameter obtained from the self-focusing effect produced by the magnetic field associated with the beam by making use of plasma equations.

The energy spectrum of an electron beam of this type has been studied in [4]. The main energy of the energy spectrum is about 0.60–0.76 of the breakdown voltage.

3. Stark broadened H_β line

The spectroscopy of line emission has been used as a basis of an important non-interfering plasma diagnostic method to determine the temperature and density of plasmas by making use of the line width and line shift of the spectral line for many years [10]. As is well known, Stark broadening and shifts caused by particle-produced fields in the plasma determine the shape of a spectral line. With temperatures in the 1–10 eV range, the dominant line broadening mechanism is Stark broadening caused by electric microfields from electrons and ions surrounding the emitting atoms or ions. The resulting Stark profiles depend almost exclusively on the electron (ion) density and are only weak functions of the temperature [11]. Due to its great Stark width, the H_β line is the most widely used for plasma diagnosis purposes [12].

Since our source is repetitive pulsed low-pressure plasma, the integrated signal technique is employed to record the line profile on a charged couple device. The transient DDPEBG device produces high electromagnetic noises so that the spectra are transferred by a fibre cable to the Oriel monochromator.

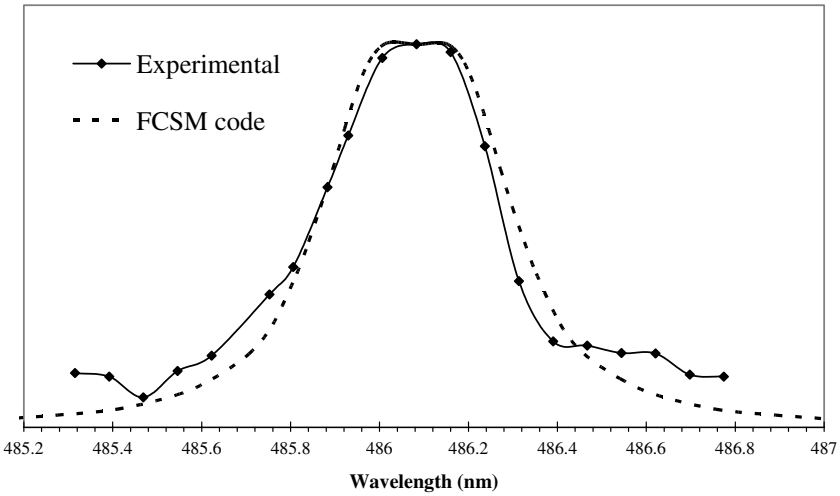

Figure 6. The line profile of the H_β line and the solid line is the result of the FCSM model at 2.5 eV and 3.16×10^{21} m^{-3} electron temperature and density, respectively.

The spectra emitted by the electron beam generator are observed in the side-on direction at the exit of anode A_2. Details of the experimental arrangement can be found in [13]. The working gas was helium where the H_β line is observed in the experimental spectrum, due to hydrogen present as an impurity in the helium, and was sufficiently strong for reasonable line profiles to be obtained. The H_β line emitted from the DDPEBG is recorded using a 1200 lines mm^{-1} grating on a Hamamatsu CCD. The wavelength calibration of our measured spectra and the determination of the instrumental width were done by He, Cd, Na spectral lamps and a He–Ne laser. The comparison of the Stark width of the H_β line with the result of the numerical code of the full computer simulation method (FCSM) [14] is given in figure 6.

In the figure the dotted lines show the experimental line profile of the H_β, and the solid one indicates the same line from the numerical code of the FCSM at 2.5 eV and 3.16×10^{21} m^{-3} electron temperature and density, respectively. To obtain the pure Stark width experimentally, deconvolution procedure takes place after subtracting the contribution originating from Doppler and instrumental broadening as given in [15]. At the end, the pure Stark FWHM is obtained experimentally as 4.48 ± 0.46 Å.

The electron density is determined by using FWHM of the H_β line as given in [16]. For a temperature range 1–4 eV and for densities between 10^{20} and 10^{24} m^{-3}, it is

$$N_e = 1.09 \times 10^{22} (\Delta\lambda_{1/2})^{1.458}\ \mathrm{m}^{-3}, \tag{2}$$

where the full half width $\Delta\lambda_{1/2}$ is in nanometres.

As given in equation (2), the electron density for the obtained Stark FWHM is $3.38(\pm 0.5) \times 10^{21}$ m^{-3}.

4. Pinch effect of the beam

Once the channel has been developed the beam follows the same path, even at higher current intensities, creating the supplementary ionization necessary for charge neutralization of the beam self-field. Furthermore, a strong self-focusing effect is established due to the magnetic field produced by the fast and narrow electron beam, which is called 'cylindrical pinch'. Here, the magnetic field is azimuthal (i.e. $\boldsymbol{B}_\theta$ only), while the plasma current is axial (i.e. j_z only), as shown in figure 7 [17, 18].

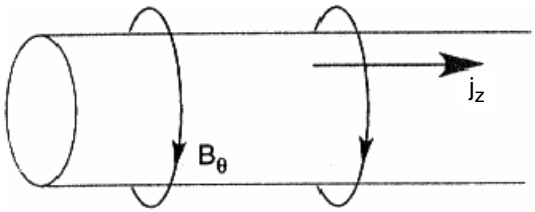

Figure 7. Cylindrical pinch equilibrium with azimuthal $\boldsymbol{B}_\theta$ field created by an axial plasma current j_z.

The steady-state solution of the magnetohydrodynamic (MHD) equations, in the case of isotropic pressure, for both the plasma and magnetic field must satisfy the three equations

$$\nabla_p = \boldsymbol{j} \times \boldsymbol{B}, \qquad \nabla \cdot \boldsymbol{B} = 0, \qquad \nabla \times \boldsymbol{B} = \mu_0 \boldsymbol{j}. \tag{3}$$

Substituting for $\boldsymbol{j}$ from Ampere's law into the force-balance equation and after some manipulation of this set of equations, we obtain for the radial dependence of pressure [17]

$$p(r) = p_0 - \frac{B_\theta^2(r)}{2\mu_0} - \frac{1}{\mu_0}\int_0^r \frac{B_\theta^2}{r}\mathrm{d}r, \tag{4}$$

where p_0 is the (peak) pressure assumed in this case to occur at $r = 0$. In a plasma column, we have $j_z(r) = j_{z_0}$ for $r < a$ and $j_z\ (r) = 0$ for $r > a$, with a denoting the plasma column radius, allowing therefore a total plasma current $I = \pi a^2 j_{z_0}$. Assuming the current density within the plasma uniform, then by Ampere's law the magnetic field strength B_θ is proportional to the radius r, so that we may write $B_\theta = B_{\theta a}\, r/a$. Carrying out the integral over r in equation (4), within $r < a$, we obtain the following dependence for the pressure:

$$p(r) = p_0 - \frac{B_{\theta a}^2 r^2}{\mu_0 a^2}, \tag{5}$$

where $B_{\theta a}$ is the azimuthal field at the edge of the plasma related to the total current by $B_{\theta a} = \mu_0 I/2\pi a$. We see that

Table 2. Typical parameters of the DDPEBG.

Maximum electron energy (keV), V_b	20
Mean electron energy (keV)	0.60–0.76 × V_b
Beam energy (mJ)	1–20
Pulse duration FWHM (ns)	50–100
Average beam diameter (μm)	4–10
Peak current (A)	1–20
Peak current density (A cm^{-2})	10^6
Peak power density (W cm^{-2})	10^{10}

the pressure profile has a parabolic dependence on radius r. Since the pressure must vanish at the edge of the plasma, i.e. $p(a) = 0$, we still have

$$p_0 = \frac{B_{\theta a}^2}{\mu_0} = \frac{\mu_0 I^2}{4\pi^2 a^2}. \tag{6}$$

This is known as the 'pinch condition' describing a magnetically self-constricted current-carrying plasma. From (5) and (6), we have for $r < a$

$$p(r) = p_0 \left(1 - \frac{r^2}{a^2}\right). \tag{7}$$

Defining now the average pressure on the plasma column $\bar{p}$, we may write

$$\bar{p} = \frac{2}{a^2} \int_0^a p(r) r \, \mathrm{d}r = \frac{p_0}{2} \tag{8}$$

and therefore the radius of the plasma column is given by

$$a = \sqrt{\frac{\mu_0 I^2}{4\pi^2 p_0}} = \frac{I}{\pi} \sqrt{\frac{\mu_0}{8\bar{p}}}. \tag{9}$$

The radius of the filamentary discharge depends only on the discharge current and pressure. The electron pressure for the evaluated electron temperature and density is equal to 9.5 Torr which is two orders of magnitudes higher than the gaseous one. For the conditions of our experiment $I = 0.6$ A and $p = 9.5$ Torr, so that the plasma radius is approximately 2.1 μm. The difference between the calculated and measured value of the diameter of the beam is interpreted in the following section.

5. Discussions and conclusions

As is seen in the previous section, the calculated radius of the electron beam at 0.6 A is 2.1 μm, while the corresponding measured value is 4 μm . The difference between experimental and predicted values of the beam diameter can be explained as follows: first, the most energetic electrons of the beam are positioned in the middle of it; second, on the upper surface of the material there is a raised ridge formed by the molten material pushed upward by the pressure of the evaporating material, while on the surface of the material adjoining the hole there are refrozen globules of material from the hole, as can be seen in figure 5 [19, 20].

Typical parameters of the DDPEG are given in table 2 and the particle density of the beam, evaluated for a 2.1 μm beam radius with 0.6 A, is 3.38(±0.5) × 10^{21} m^{-3}.

Changes in power by a factor of 100 or more can be achieved by simply changing the accelerating voltage, which indicates that the same e-beam device may be used in many applications. The DDPEBG operates without any contact with an insulator surface and that is why long-term operation is possible with the device. The characteristics of the electron beam generated as a result of this technique, such as its small diameter, high peak current and short pulse length, might be useful in many applications such as micro-processing [21], x-ray generation, high-power laser pre-ionization and thin film deposition [22].

Acknowledgments

We would like to thank W Olchawa for supplying us the H_β line profiles corresponding to our plasma conditions and R Turan for supplying the spectroscopic equipment.

References

[1] Mingolo N, Gonzalez C R, Martinez O E and Rocca J J 1997 *J. Appl. Phys.* **82** 4118
[2] Frank K and Christiansen J 1989 *IEEE Trans. Plasma Sci.* **17** 748
[3] Udrea M V, Pointu A M, Modreanu G, Ganciu M, Popescu I I and Mandache N B 1997 *J. Phys. D: Appl. Phys.* **30** L33
[4] Modreanu G, Mandache N B, Pointu A M, Ganciu M and Popescu I I 2000 *J. Phys. D: Appl. Phys.* **33** 819
[5] Goktas H, Oke G, Esendemir A and Udrea M 2003 *Turk. J. Phys.* **27** 72–82
[6] Schaefer G and Schoenbach K H (ed) 1989 *Basic Mechanism Contributing to the Hollow Cathode Effect* (*NATO ASI Series B: Physics* vol 219) (New York: Plenum) pp 55–77
[7] Kolobov V I and Tsendin L D 1995 *Plasma Sources Sci. Technol.* **4** 551
[8] Grechanyi V G and Metel A S 1982 *Sov. Phys.—Tech. Phys.* **27** 284
[9] Metel A S 1985 *Sov. Phys.—Tech. Phys.* **30** 1133
[10] Griem H R 1974 *Spectral Line Broadening by Plasmas* (New York: Academic)
[11] Berg H F, Ali A W, Lincke R and Griem H R 1962 *Phys. Rev.* **125** 199
[12] Gigosos M A and Cardenoso V 1996 *J. Phys. B: At. Mol. Opt. Phys.* **29** 4795
[13] Goktas H, Demir A, Kacar E, Oke G, Turan R and Seyhan A 2005 *Eur. Phys. J. Appl. Phys.* submitted
Goktas H, Demir A, Turan R, Seyhan A and Oke G 2003 Measurements and modelling of neutral helium spectral lines emitted from electron beam generator *Proc. Int. Conf. Plasma 2003: Research and Applications of Plasmas* (Warsaw, 8–12 September 2003)
[14] Olchawa W, Olchawa R and Grabowski B 2004 *Eur. Phys. J.* D **28** 119
[15] Kelleher D 1981 *J. Quant. Spectrosc. Radiat. Transfer* **25** 191
[16] Kunze H J, Proud J M and Luessen L H (ed) 1986 *Radiative Processes in Discharge Plasmas* (New York: Plenum)
[17] Goldston R J and Rutherford P H 1995 *Introduction to Plasma Physics* (Britol: Institute of Physics Publishing)
[18] Rose D J and Clark M 1961 *Plasmas and Controlled Fusion* (Cambridge, MA: MIT Press)
[19] Bakish R 1962 *Electron Beam Technology* (New York: Wiley)
[20] Meleka A H 1971 *Electron-Beam Welding* (New York: McGraw-Hill)
[21] Goktas H, Udrea M, Kirkici H and Oke G 2002 *IEEE Trans. Plasma Sci.* **30** 1837
[22] Goktas H, Oke G, Udrea M and Esendemir A 2002 *Czech. J. Phys.* **52** D756